

## Application of Fourier Transform Infrared Microspectroscopy (FTIR) and Thermogravimetric Analysis (TGA) for quick identification of Chinese herb *Solanum lyratum*

Yiling Wang

College of Life Science, Shanxi Normal University, 041004 Linfen, China

\*Corresponding author: ylwangbj@yahoo.com.cn

### Abstract

*Solanum lyratum* is a medicinal plant used to treat cancers and tumors. The objective of this study was to apply Fourier transform infrared microspectroscopy (FTIR) and thermogravimetric analysis (TGA) to quick identification of *S. lyratum* fourteen samples from its main geographic origins in China. The hierarchical dendrogram based on principal component analysis (PCA) of FTIR and TGA data showed that these samples could be divided into three ecotypes according to their geographic distances to the ocean: inland type, middle type and inshore type. Differences in cell compositions and structures by FTIR and TGA indicated that higher content of cell wall polysaccharides, hermo-oxidative degradation of hemicellulose (HODH) and degradation of lignin (DL) are appointed for inshore type compared to inland type and middle type. These indices (cell wall polysaccharides, HODH and DL) can be characteristic values for identifying *S. lyratum* from different region in China. The FTIR-TGA method, providing compositional and structural differences in their macromolecules in cell for the herbs rapidly and accurately, would be capable of further identification of other Chinese medicinal plant.

**Keywords:** *Solanum lyratum*; Solanaceae; infrared spectroscopy; thermogravimetric analysis; distinct geographical origin.

**Abbreviations:** FTIR-fourier transform infrared microspectroscopy; TGA-thermogravimetric analysis; PCA-principal component analysis; HODH-hermo-oxidative degradation of hemicellulose; DL-degradation of lignin; DC-degradation of cellulose.

### Introduction

*Solanum lyratum* Thunb. (Solanaceae), well-known as "White-floss-Bine" in China, has long been one of the most valued traditional medicines in oriental countries. This plant has been used as traditional drugs for treating cancer, tumour and allergy (Lee et al., 1997; Kang et al., 1998; Graham et al., 2000), and also described as being antioxidant (Kuo et al., 2009), inducing cytotoxicity and apoptosis (Hsu et al., 2008; Ikeda et al., 2003; Lee et al., 2009; Sun et al., 2006). Therefore, increasing commercial interest is exposed to this herb for its valuable properties. Commercial herbs collected from a single origin would significantly cause resource depletion (Williams et al., 2007). However, the diverse geographical origins of *S. lyratum* lead to some difficulties in the marketing chains of this herb. Although a plant can be easily identified by its morphological characteristics, it is not always possible to characterize the herb from the dry portion of stems. Thus, a simple and rapid method for determination of *S. lyratum* is highly required. During the past years, there has been a growing interest in combining or merging data obtained from different instruments since it is believed to increase quality of information about the studied samples (Rudnitskaya et al., 2006). Fourier transform infrared microspectroscopy (FTIR) and thermogravimetric analysis (TGA) (Caine et al., 2012; Cheung et al., 2011; Duband et al., 2012) are two widely applied analytical techniques. FTIR is an alternative non-destructive analytical technique that allows the reliable, direct and fast determination of several properties without any sample pretreatment. The entire FTIR spectra of an organic compound provide a unique fingerprint, which can be readily distinguished from the FTIR absorption pattern of other compounds (Popescu et al., 2007). Moreover, characteristic absorption bands can be used for compound-specific detection (Mehrotra et al., 2007; Menczel

and Prime, 2009; Roy et al., 2009; Antonakos et al., 2007). Nowadays, FTIR has become a tool of versatility in plant science of biochemical and molecular biology (Schwinte et al., 2008), ecology (Lang et al., 2009), physiology (Oliveira et al., 2008) and agriculture (Artz et al., 2008). This technology has also been used in plant classification and identification at levels of genus, section, species and even cultivar (Zhu et al., 2004; Shen et al. 2008; Tapp et al., 2003; Lu et al., 2008). In another way, TGA has the advantage that it is rapid, reliable, reproducible and good at control over the temperature and heating rate. They have been used to assay the chemical compositions and structures of the sample (Menczel and Prime, 2009). Nowadays, this technology has been applied to the thermal analysis of energy compounds such in plant such as lipid (Garcia et al., 2007) and polysaccharides (Zhang et al., 2009; Munir et al., 2009), and also for plant classification and identification (Ross et al., 2008). These studies have shown that FTIR and TGA provide a considerable amount of information for identifying *S. lyratum* of diverse geographical origin. In this research, FTIR and TGA are conducted to investigate the structural and compositional variations of some homologous macromolecules contained in this herb. We showed that this technique could be applied in the future as a valid method to distinguish the authentication of medicines.

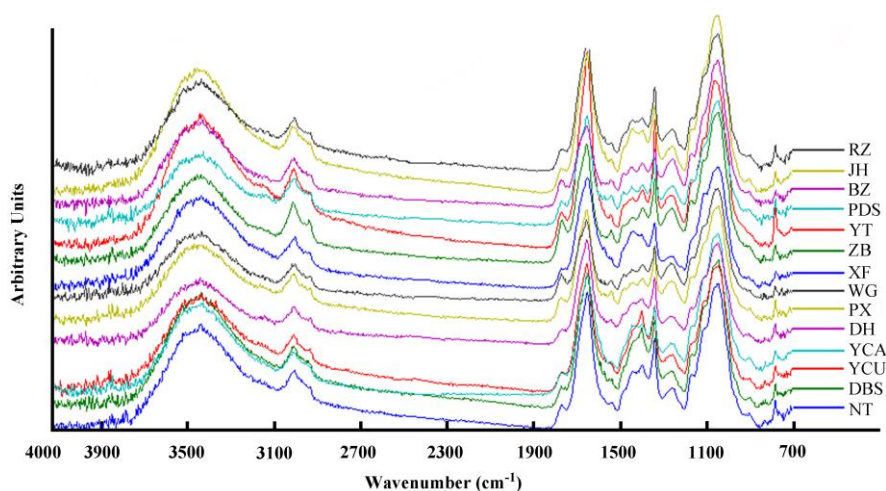
### Results and discussions

#### *The properties of FTIR spectra curve and cluster analysis*

FTIR spectroscopy has been shown to be a valuable tool for differentiating and classifying closely related species. With this technique used in plant, Kim et al. (2004) reported that

**Table 1.** General band assignments of the average FTIR spectrum of plants based on the literature.

Frequency (cm <sup>-1</sup> )	Definition of the Spectral Assignments
1	3380 O-H and N-H group stretching vibration: carbohydrates protein 2957 CH <sub>3</sub> asymmetric stretching: mainly lipids with a little contribution from proteins, carbohydrates, and nucleic acids
2	2922 CH <sub>2</sub> asymmetric stretching: mainly lipids with a little contribution from proteins, carbohydrates, and nucleic acids 2873 CH <sub>3</sub> asymmetric stretching: mainly proteins with a little contribution from lipids, carbohydrates, and nucleic acids
3	2862 CH <sub>2</sub> asymmetric stretching: mainly lipids with a little contribution from proteins, carbohydrates, and nucleic acids
4	1733 Saturated ester C=O stretch: phospholipids, cholesterol esters, hemicellulose, and pectin 1622 Amide I (protein C=O stretch): protein and pectin 1601 C=O aromatic stretching: lignin 1546 Amide II (C=N and N-H stretching): mainly proteins 1458 Amide III (aromatic hydrocarbons): mainly proteins
5	1452 C-H: cell wall polysaccharides
6	1420 O-H bending: cell wall polysaccharides, alcohols, and carboxylic acids
7	1380 C-H bending of aliphatic CH <sub>2</sub> : cell wall polysaccharides
8	1320 N-acetylglucosamine: chitin and chitosan
9	1250 Pectic substances 1235 Amide IV (C=N and N-H stretching): mainly proteins
10	1160 Symmetric bonding of aliphatic CH <sub>2</sub> , OH, or C-O stretch of various groups: cell wall polysaccharides
11	1145 Cellulose (β-1.4 glucan)
12	1101 Antisymmetric in-phase: pectic substances 1073 Rhamn ogalactorunan. b-galactan 1064 C-O stretching: cell wall polysaccharides (glucomannan)
13	1035 OH and C-OH stretching: cell wall polysaccharides (arabinan)
14	895 Arabinan 893 Galactan
15	873 B-D-Fructose

**Fig 1.** FTIR spectra in the range 4000 - 700 cm<sup>-1</sup> obtained from stems of *S. lyratum* fourteen samples.

FTIR could successfully exploit for determining phylogenetic relationships between flowering plants. Lu et al. (2004) used this method to identify the species in *Hypericum* and *Triadenum*. Gorgulu et al. (2007) revealed FTIR spectroscopy could be successfully applied to differentiate genera *Ranunculus*, *Astragalus* and *Acantholimon*. In our study, similar infrared spectral patterns and wave-number of absorbing peaks were demonstrated in stem samples collected from different geographic regions (Fig 1). As shown in the figure, they are complex spectra representing many different functional groups of lipids and carbohydrates. The positions and assignments of the bands are listed in Table 1. These results imply that *S. lyratum* samples of different geographic origins have almost the same functional

groups, and suggest that these herbs might have the same usage in medical treatment (Singh et al., 2010). However, differences in several main bands can't be ignored. Their relative intensities and the band positions exhibited variations. In addition, many weak FTIR bands are observed which may be used as markers for the samples originating from different geographic regions (Tonder and Wyk, 2007). Hierarchical clustering obtained by the PCA data of FTIR bands contained in the 700-4000 cm<sup>-1</sup> region is used as a classification method, resulting in the dendrogram displayed in Fig 2b. Obviously, this dendrogram didn't consist with the origins' latitudes and longitude (Fig 2a) whatever similarity score circumscriptions being selected. However, if the sea is taken into consideration, the distances between these origins and the sea agreed well

**Table 2.** Comparison on three selected pyrolytic parameters of *Solanum lyratum* samples of three types.

	Type I	Type II	Type III
HODH	23.52±3.91a	53.69±4.87b	51.39±4.58b
DC	21.31±2.95a	22.84±1.18a	19.51±3.20a
DL	1.32±0.04b	6.11±1.62a	4.42±1.98a

HODH, hermo-oxidative degradation of hemicellulose. DC, degradation of cellulose. DL, degradation of lignin. Test of significance is performed by REGWQ's multiple comparison test, at 0.05 level of significance, values with the same letter are not significantly different.

**Table 3.** Localities and number of sample of *S. lyratum*.

No	Sample	Locality	Longitude	Latitude	Altitude(m)	
1	PDS	20	Pingdingshan, Henan	113°17'	33°44'	1200
2	DH	20	Donghai, Jiangsu	120°19'	32°51'	1000
3	NT	20	Nantong, Jiangsu	120°51'	32°01'	800
4	PX	20	Pingxiang, Jiangxi	113°50'	27°37'	1200
5	YT	20	Yingtian, Jiangxi	117°03'	28°14'	1500
6	DBS	20	Dabieshan, Anhui	112°40'	30°10'	1500
7	WG	20	Wugang, Henan	113°30'	33°17'	950
8	JH	20	Jinhua, Zhejiang	119°14'	28°32'	900
9	YCU	20	Yongchun, Fujian	117°41'	25°13'	1000
10	XF	20	Xiangfan, Hubei	112°08'	32°02'	1000
11	ZB	20	Zibo, Shandong	118°03'	36°48'	800
12	YCA	20	Yichang, Hubei	111°17'	30°42'	890
13	BZ	20	Bozhou, Anhui	115°47'	33°52'	1100
14	RZ	20	Rizhao, Shandong	119°32'	35°23'	950

with the dendrogram (circumscriptions similarity score: -0.3): WG, XF and YCA, which had the largest distances among all the origins, could be classified into one population; PX, YT, JH, BZ, PDS and DBS, which had the moderate distances, could be grouped into another population; ZB, DH and NT, which are all inshore cities, could be classified into the third population. Then, it seemed that RZ and YCU were the fourth and fifth types, respectively. Since both RZ and YCU are inshore cities, they were merged into the same type with ZB, DH and NT.

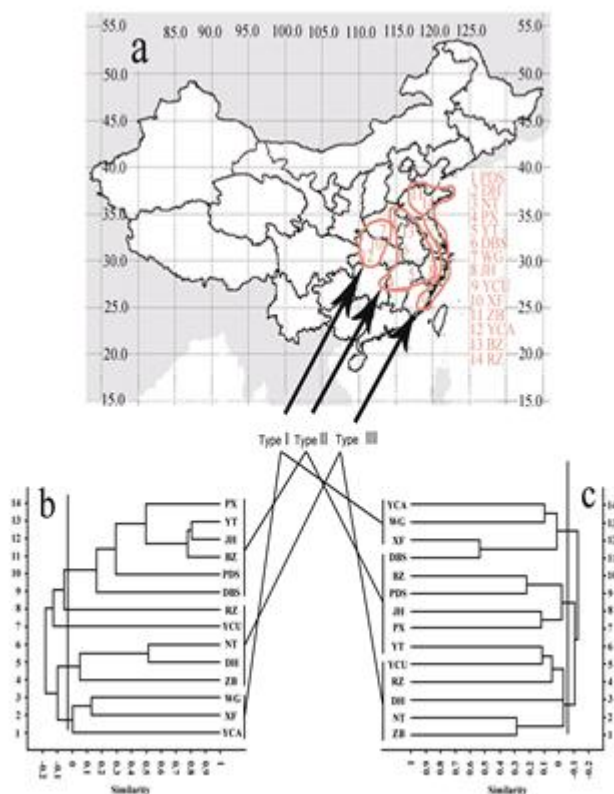
#### The properties of TGA curve and cluster analysis

Fig. 3 shows the thermogram illustrating recorded TGA. Samples from all regions manifest concordant thermal degradation characteristics. Similar Z-shaped TGA curves were obtained for all samples. It showed a three-stage weight loss below 500 °C. The first minor one corresponded to the loss of water around 80 °C, while the others to macromolecule decomposition. Dendrogram of TGA cluster analysis (Fig 2c) was obtained using the PCA data of total TGA bands. Compared with FTIR cluster in Fig 2b, most of the origins had the same ascriptions of population except DBS and YT. For more expedient analysis, these two origins were merged into the second cluster (Fig 2c). Then, it is in good agreement with the results in the FTIR clusters and geographic conditions (Fig 2a). These results indicated that the distances of the origins to the ocean significantly affect the population type (or ecotype). Here we suggest classifying all these origins into three types: Type I— inland type which is very far from the sea, Type II — middle type which also has a long but shorter distance than Type I to the sea, and Type III — inshore type which is beside the sea, since it will do some help in studying and utilizing this herb.

#### The characterization and differentiation of three ecotypes in molecular conformation

In order to investigate the structural and compositional variations of macromolecules of this herb from different regions, detailed spectral analyses were additionally

performed (Table 1). Fig. 4 showed all bands of the average infrared spectra of Type I, Type II, and Type III. They were divided into three distinct frequency regions: (1) 3950–2800  $\text{cm}^{-1}$  — the O–H stretching modes of polysaccharides and intermolecular H bonding (Yang and Yen, 2002); (2) 3050–2800  $\text{cm}^{-1}$  — this region contains two bands, in which the  $\text{CH}_2$  symmetric and asymmetric stretching bands are mainly due to lipids (Mantsch and Chapman, 2009); (3) 2000–700  $\text{cm}^{-1}$  (fingerprint region) (Lu et al., 2008) — cell wall polysaccharides which have different combinations and glycosidic linkages of the monosaccharides. In region (1), the spectra are normalized with respect to the O–H stretching modes, which are observed around 3380  $\text{cm}^{-1}$ . Results show that, the intensity values of the carbohydrates band of Type I ( $1.61 \pm 0.03$ )  $\times 10^{-2}$  is lower than Type II ( $1.84 \pm 0.12$ )  $\times 10^{-2}$  ( $p < 0.05$ ) and Type III ( $0.1.93 \pm 0.07$ )  $\times 10^{-2}$  ( $p < 0.05$ ). This indicated possible differences in the concentration of polysaccharides present in the samples. In region (2), significant differences were only found in  $\text{CH}_2$  asymmetric stretching bands among above mentioned three bands. Our results revealed that the intensity values for the band around 2922  $\text{cm}^{-1}$  was at a higher value for Type I ( $1.32 \pm 0.04$ )  $\times 10^{-2}$  when compared to Type II ( $1.11 \pm 0.06$ )  $\times 10^{-2}$  ( $p < 0.05$ ), and for the band around 2862  $\text{cm}^{-1}$ , Type I ( $0.92 \pm 0.06$ )  $\times 10^{-2}$  was higher than Type II ( $0.79 \pm 0.04$ )  $\times 10^{-2}$  ( $p < 0.05$ ). It implies that Type I may have higher content of lipids than Type III. And in the fingerprint region, the trend that intensity values increased from the inland type (Type I) to inshore type (Type II) is so similar to the two aforementioned distinct frequency regions. For example, as to the band around 1452  $\text{cm}^{-1}$  which was attributed to the aliphatic C–H group, the intensity values increased from the inland type ( $0.70 \pm 0.06$ )  $\times 10^{-2}$  to inshore type ( $0.87 \pm 0.09$ )  $\times 10^{-2}$ , while Type III had the middle values ( $0.85 \pm 0.11$ )  $\times 10^{-2}$ . All these results suggest that the inshore type has higher content of cell wall polysaccharides. To verify the above-mentioned trends of polysaccharides contained in samples of the three types, The average TGA of three types was additionally performed for each region, simultaneously (Fig. 5). The compound started to lose water at about 80 °C and the loss continued up to about 120 °C. The TGA curve showed a sharp slope up to



**Fig 2.** The main origins of *S. lyratum* are located at the East, South and Central China (a). Phenograms obtained from the UPGMA cluster analysis using the data of FTIR (b) and TGA (c) showed these geographic regions could be divided into three types: Type I— inland type, Type II — middle type and Type III — inshore type.

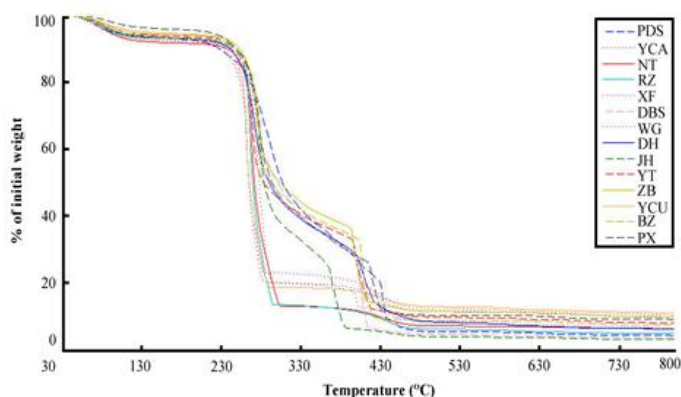


**Fig 3.** Thermogram resulting from analysis of *S. lyratum* samples from 14 geographic regions, obtained under a nitrogen flow of 50 ml/min, heating rate of 10 °C /min.

about 280 °C. This weight loss may be attributed to the weight of two ammonia molecules, one being bonded to an  $\alpha$ -carbon atom and the other attached to the carbon atom of the guanidyl group (Mallik and Kar, 2005). The main decomposition of the polysaccharides started above 200 °C with the evolution of carbon dioxide (Zohuriaan and Shokrolahi, 2004). This decomposition process continued up to about 480 °C with the removal of almost all the compound as gaseous products. Those thermal events were designated

as: evaporation of residual moisture, 85 ~ 125 °C; hermo-oxidative degradation of hemicellulose (HODH), 245 ~ 280 °C; degradation of cellulose (DC), 280 ~ 325 °C; degradation of lignin (DL), 350 ~ 440 °C (Welch et al., 2007). The selected three pyrolytic parameters of the three types tested are presented at Table 2. Results showed that the HODH values of Type I ( $23.52 \pm 3.91$ ) was lower than Type II ( $53.69 \pm 4.87$ ) ( $p < 0.05$ ) and Type III ( $51.39 \pm 4.58$ ) ( $p < 0.05$ ). The DL value of Type I ( $1.32 \pm 0.04$ )  $\times 10^{-2}$  was lower than Type II ( $6.11 \pm 1.62$ ) ( $p < 0.05$ ) and Type III ( $4.42 \pm 1.98$ ) ( $p < 0.05$ ). But the DC values of these three types displayed no significant difference. These results verify the conclusion drawn from spectral analyses that the inshore type has higher content of cell wall polysaccharides. What's more, cell wall polysaccharides, HODH and DL are useful characteristic values for identifying *S. lyratum* in various regions.

## Materials and methods

### Apparatus

A Magna FTIR 750 spectrometer from Nicolet (Madison, WI, USA), equipped with a DTGS temperature-stabilized detector, a KBr beam splitter and a benchmark out-of compartment overhead attenuated total reflectance accessory with a flow-through top-plate fitted with 45° ZnSe 6 reflection crystal from Graseby Specac (Orpington, UK), was used to collect the ATR-FTIR spectra of the different samples analyzed. For TGA procedure, an automatic recording thermobalance (Mettler-Teledo TGA/SDTA 851° instruments, Switzerland) was used in this study.

Acquisition and preprocessing of data from above-mentioned two apparatus were carried out with their custom-built software Omnic 7.0 and STAR<sup>e</sup>, respectively.

### Samples collection and pretreatment

*S. lyratum* samples were collected from its main geographical distribution in China. Among these samples, geographic regions covered eight provinces including fourteen cities (Table 3, Fig 2a): Zibo (ZB) and Rizhao (RZ) in Shandong Province, Donghai (DH) and Nantong (NT) in Jiangsu Province, Bozhou (BZ) and Dabieshan (DBS) in Anhui Province, Pingdingshan (PDS) and Wugang (WG) in Henan Province, Xiangfan (XF) and Yichang (YCA) in Hubei Province, Pingxiang (PX) and Yingtian (YT) in Jiangxi Province, Yongchun (YCU) in Fujian Province, and Jinhua (JH) in Zhejiang Province. In each sample location, 20 healthy and mature individuals were randomly chosen. Fully mature *S. lyratum* stems were excised from plants and freeze-dried immediately. The samples were then pulverized by light grinding in a mortar and stored at  $-20$  °C until the subsequent use.

### FTIR and TGA procedures

FTIR procedure was conducted following the methods of Lu et al. (2004) with some modifications. A small amount of powdered stem was placed on the ZnSe crystal. Constant pressure was applied onto the samples ensuring good contacts between the crystal and the sample. The absorbance spectra of each sample were the mean of 32 scans collected over the wave number ranged from 4,000  $\text{cm}^{-1}$  to 700  $\text{cm}^{-1}$ , with a resolution of 2  $\text{cm}^{-1}$ . The reference spectra were acquired from the cleaned blank crystal prior to the presentation of each sample replicate. The collection time for

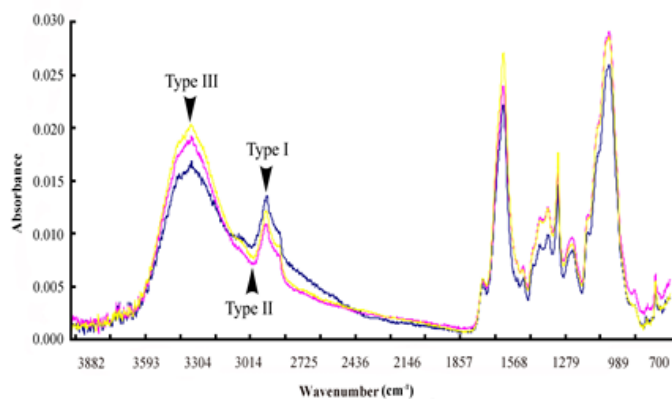


**Fig 4.** The average FTIR spectra in the 4000 and 700  $\text{cm}^{-1}$  region of Type I, Type II and Type III obtained by the cluster analysis.

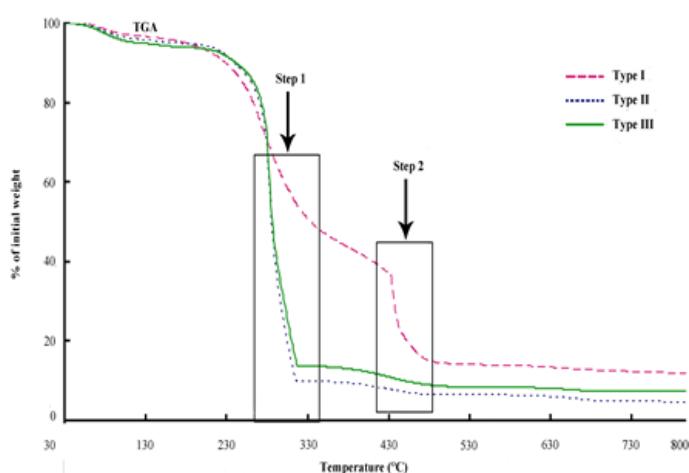


**Fig 5.** The average TGA curves of Type I, Type II and Type III from 30 to 800  $^{\circ}\text{C}$ . Thermal events are designated as: 85–125  $^{\circ}\text{C}$ , evaporation of residual moisture; 245–280  $^{\circ}\text{C}$ , thermo-oxidative degradation of hemicellulose; 280–325  $^{\circ}\text{C}$ , degradation of cellulose; 350–440  $^{\circ}\text{C}$ , degradation of lignin.

each sample spectrum was 60 s. Samples were run in triplicate, all of which were undertaken within a single day. For TGA procedure, about 5 mg of lyophilized sample was analyzed in the temperature interval 30–800  $^{\circ}\text{C}$  with a constant heating rate of 10  $^{\circ}\text{C}/\text{min}$ , under a nitrogen flow of 50 ml/min. The presence of oxygen enhanced the thermal decomposition of materials at lower temperatures, caused gas-phase reactions with the released volatiles, and promoted combustion of char residue (Francioso et al., 2005). The results of TGA analysis were expressed on a dry weight basis because it facilitated the comparison among different samples. The average of three TGA runs was reported for samples of each geographic region. The TGA curve of each run was automatically corrected with the baseline of a blank experiment (Brown, 2001).

#### Data analyses

Before analysis, a set of preprocessing steps should be implemented on the raw dataset. Wbmpen's de-noise treatment was performed by wavelet procedure in MatLab (Version 7.0). These de-noise data were handled with 2nd derivate, 5 points smoothing and peak normalization by the Unscrambler procedure (the 9.7 package). These data were

then subjected to multivariate analysis. Principal component analysis (PCA) was performed to reduce the dimensionality. For UPGMA clustering of FTIR and TGA by PAST procedure (Version 1.68), 10 components (accounting for 95% of the total variances) of FTIR and 12 components (accounting for 95% of the total variances) of TGA were selected from PCA, respectively. REGWQ's multiple comparison test ( $P = 0.05$ ) was applied in order to detect differences in some selected TGA data by SAS 9.0.

#### Conclusion

In conclusion, our study showed that the combined use of FTIR and TGA provides an excellent approach for the fully mechanized analysis of *S. lyratum* herbs. The hierarchical dendrograms based on PCA of FTIR and TGA data, showed that *S. lyratum* of all geographic regions could be divided into three ecotypes: inland type, middle type and inshore type. Moreover, hierarchical dendrogram clusters herbal medicines into different groups, clearly showing that this method can adequately discriminate different herbal medicines using FTIR and TGA data. Differences in cell compositions and structures by FTIR and TGA indicated that inshore type have higher cell wall polysaccharides, HODH and DL. Accordingly, these indices appear useful for discriminating closely related varieties of *S. lyratum*, and the combination of FTIR and TGA techniques can be potentially used for quick identification and classification of other plants.

#### Acknowledgements

This research was supported by the funding of the Natural Science Foundation of Shanxi Province (2011011031-2).

#### References

- Antonakos A, Liarokapis E, Leventouri T (2007). Micro-Raman and FTIR studies of synthetic and natural apatites. *Biomaterials* 28: 3043-3054.
- Artz RRE, Chapman SJ, Robertson JAH, Potts JM, Defarge FL, Gogo S, Comont L, Disnar JR, Francez AJ (2008). FTIR spectroscopy can be used as a screening tool for organic matter quality in regenerating cutover peatlands. *Soil Biol Biochem* 40: 515-527.
- Brown, ME (2001). Introduction to Thermal analysis: Techniques and Applications. 2th ed. The Netherlands: Kluwer Academic Publishers.
- Caine S, Heraud P, Tobin MJ, McNaughton D, Bernard CC (2012). The application of Fourier transform infrared microspectroscopy for the study of diseased central nervous system tissue. *Neuroimage* 59(4):3624-3640.
- Cheung KT, Trevisan J, Kelly JG, Ashton KM, Stringfellow HF, Taylor SE, Singh MN, Martin-Hirsch PL, Martin FL (2011). Fourier-transform infrared spectroscopy discriminates a spectral signature of endometriosis independent of inter-individual variation. *Analyst* 136: 2047-2055.
- Duband S, Govin A, Dumollard JM, Forest F, Basset T, Péoc'h M (2012). Laryngeal teflonoma identified by Fourier-transform infrared microspectroscopy after forensic autopsy: an interesting tool for foreign material identification in forensic cases. *Forensic Sci Int* 214(1-3):e26-9.
- Francioso O, Montecchio D, Gioacchini P, Ciavatta C (2005). Thermal analysis (TG-DTA) and isotopic characterization ( $^{13}\text{C}$ - $^{15}\text{N}$ ) of humic acids from different origins. *Appl Geochem* 20: 537-544.

- Garcia CC, Franco PIBM, Zuppa TO, Filho NRA, Leles MIG (2007). Thermal stability studies of some cerrado plant oils. *J Therm Anal Calorim* 87: 645-648.
- Gorgulu ST, Dogan M, Severcan F (2007). The characterization and differentiation of higher plants by fourier transform infrared spectroscopy. *Appl Spectrosc* 61: 300-308.
- Graham JG, Quinn ML, Fabricant DS, Farnsworth NR (2000). Plants used against cancer – an extension of the work of Jonathan Hartwell. *J Ethnopharmacol* 73:347-377.
- Hsu SC, Lu JH, Kuo CL, Yang JS, Lin MW, Chen GW, Su CC, Lu HF, Chung JG (2008). Crude extracts of *Solanum lyratum* induced cytotoxicity and apoptosis in a human colon adenocarcinoma cell line (Colo 205). *Anticancer Res* 28: 1045-1054.
- Ikedda T, Tsumagari H, Honbu T, Nohara T (2003). Cytotoxic activity of steroidal glycosides from *Solanum* plants. *Biol Pharm Bull* 26: 1198-1201.
- Kang B, Lee E, Hong I, Lee J, Kim H (1998). Abolition of anaphylactic shock by *Solanum lyratum* Thunb. *Int Immunopharmacol* 19: 729-734.
- Kim SW, Ban SH, Chung H, Cho S, Chung HJ, Choi PS, Yoo OJ, Liu JR (2004). Taxonomic discrimination of flowering plants by multivariate analysis of Fourier transform infrared spectroscopy data. *Plant Cell Rep* 23: 246-250.
- Kuo WW, Huang CY, Chung JG, Yang SF, Tsai KL, Chiu TH, Lee SD, Ou HC (2009). Crude extracts of *Solanum lyratum* protect endothelial cells against oxidized low-density lipoprotein-induced injury by direct antioxidant action. *J Vasc Surg* 50: 849-860.
- Lang SI, Cornelissen JHC, Klahn T, Logtestijn RSP, Broekman R, Schweikert W, Aerts R (2009). An experimental comparison of chemical traits and litter decomposition rates in a diverse range of subarctic bryophyte, lichen and vascular plant species. *J Ecol* 97: 886-900.
- Lee JH, Lee YH, Lee HJ, Lee HJ, Lee EO, Ahn KS, Shim BS, Bae H, Choi SH, Ahn KS, Baek NI, Kim DK, Kim SH (2009). Caspase and mitogen activated protein kinase pathways are involved in *Solanum lyratum* herba induced apoptosis. *J Ethnopharmacol* 123: 121-127.
- Lee YY, Hsu FL, Nohara T (1997). Two new soladulcidine glycosides from *Solanum lyratum*. *Chem Pharm Bull* 45: 1381-1382.
- Lu HF, Cheng CG, Tang X, Hu ZH (2004). FTIR spectrum of *Hypericum* and *Triadenum* with reference to their identification. *J Integr Plant Biol* 46: 401-406.
- Lu HF, Shen JB, Lin XY, Fu JL (2008). Relevance of fourier transform infrared spectroscopy and leaf anatomy for species classification in *Camellia* (Theaceae). *Taxon* 57: 1274-1288.
- Mallik T, Kar T (2005). Growth and characterization of nonlinear optical L-arginine dihydrate single crystals. *J Cryst Growth* 285: 178-182.
- Mantsch HH, Chapman D (2009). *Infrared spectroscopy of biomolecules*. New York: John Wiley & Son Inc.
- Mehrotra R, Gupta A, Kaushik A, Prakash N, Kandpal H (2007). Infrared spectroscopic analysis of tumor pathology. *Indian J Exp Biol* 45: 71-76
- Menczel, JD., Prime, RB (2009). *Thermal analysis of polymers: Fundamentals and applications*. New York: John Wiley & Son Inc.
- Munir S, Daood SS, Nimmo W, Cunliffe AM, Gibbs BM (2009). Thermal analysis and devolatilization kinetics of cotton stalk, sugar cane bagasse and shea meal under nitrogen and air atmospheres. *Bioresource technol* 100: 1413-1418.
- Oliveira H, Barros AS, Delgadillo I, Coimbra MA, Santos C (2008). Effects of fungus inoculation and salt stress on physiology and biochemistry of *in vitro* grapevines: Emphasis on sugar composition changes by FT-IR analyses. *Environ Exp Bot* 65: 1-10.
- Popescu CM, Popescu MC, Singurel G, Vasile C, Argyropoulos DS, Willfor S (2007). Spectral characterization of eucalyptus wood. *Appl Spectrosc* 61: 1168-1177.
- Ross AB, Jones JM, Kubacki ML, Bridgeman T (2008). Classification of macroalgae as fuel and its thermochemical behaviour. *Bioresource technol* 99: 6494-6504.
- Roy B, Banerjee R, Chatterjee S (2009). Isolation and identification of poly beta hydroxybutyric acid accumulating bacteria of Staphylococcal sp. and characterization of biodegradable polyester. *Indian J Exp Biol* 47: 250-256.
- Rudnitskaya A, Kirsanov D, Legin A, Beullens K, Lammertyn J, Nicolai BM, Irudayaraj J (2006). Analysis of apples varieties – comparison of electronic tongue with different analytical techniques. *Sensor Actuat B – Chem* 28: 23-28.
- Schwinte P, Foerstendorf H, Hussain Z, Gartner W, Mroginski MA, Hildebrandt P, Siebert F (2008). FTIR study of the photoinduced processes of plant phytochrome phy using isotope-labeled bilins and density functional theory calculations. *Biophys J* 95: 1256-1267.
- Shen JB, Lu HF, Peng QF, Zheng JF, Tian YM (2008). FTIR spectra of *Camellia* sect. *Oleifera*, sect. *Paracamellia*, and sect. *Camellia* (Theaceae) with reference to their taxonomic significance. *J Syst Evol* 46: 194-204.
- Singh SK, Jha SK, Chaudhary A, Yadava RDS, Rai SB (2010). Quality control of herbal medicines by using spectroscopic techniques and multivariate statistical analysis. *Pharm Biol* 48: 134-141.
- Sun LX, Fu WW, Ren J, Xu L, Bi KS, Wang MW (2006). Cytotoxic constituents from *Solanum lyratum*. *Arch Pharm Res* 29: 135-139.
- Tapp HS, Defernez M, Kemsley, EK (2003). FTIR spectroscopy and multivariate analysis can distinguish the geographic origin of extra virgin olive oils. *J Agr Food Chem* 51: 6110-6115.
- Tonder VJH, Wyk BEV (2007). Chemical variation in selected Karoo medicinal plants. *S Afr J Bot* 73: 318.
- Welch AJ, Stipanovic AJ, Maynard CA, Powell WA (2007). The effects of oxalic acid on transgenic *Castanea dentata* callus tissue expressing oxalate oxidase. *Plant Sci* 172: 488-496.
- Williams VL, Balkwill K, Witkowski ETF (2007). Size-class prevalence of bulbous and perennial herbs sold in the Johannesburg medicinal plant markets between 1995 and 2001. *S Afr J Bot* 73: 144-155.
- Yang J, Yen HC (2002). Early salt stress effects on the changes in chemical composition in leaves of ice plant and Arabidopsis. A fourier transform infrared spectroscopy study. *Plant Physiol* 130: 1032-1042.
- Zhang L, Xie W, Zhao X, Liu Y, Gao W (2009). Study on the morphology, crystalline structure and thermal properties of yellow ginger starch acetates with different degrees of substitution. *Thermochim Acta* 495: 57-62.
- Zhu L, Shi GX, Li ZS, Kuang TY, Li B, Wei QK, Bai KZ, Hu YX, Lin JX (2004). Anatomical and chemical features of high-yield wheat cultivar with reference to its parents. *J Integr Plant Biol* 46: 565-572.
- Zohuriaan MJ, Shokrolahi F (2004). Thermal studies on natural and modified gums. *Polym Test* 23: 575-579.